• Basic Research •

Heparanase-1 is downregulated in chemoradiotherapy orbital rhabdomyosarcoma and relates with tumor growth as well as angiogenesis

Wei-Qiang Tang[1], *Yan Hei*[2], *Jing Lin*[3]

[1]Department of Ophthalmology, the Fourth Medical Centre, Chinese PLA General Hospital, Beijing 100048, China
[2]Department of Ophthalmology, the Third Medical Centre, Chinese PLA General Hospital, Beijing 100039, China
[3]Department of Clinical Laboratory, the Fourth Medical Centre, Chinese PLA General Hospital, Beijing 100048, China
Correspondence to: Jing Lin. Department of Clinical Laboratory, the Fourth Medical Centre, Chinese PLA General Hospital, No. 51 Fucheng Road, Beijing 100048, China. lin_jing_bj@163.com
Received: 2021-02-09 Accepted: 2021-08-20

Abstract

● **AIM:** To determine the role of heparanase-1 (HPSE-1) in orbital rhabdomyosarcoma (RMS), and to investigate the feasibility of HPSE-1 targeted therapy for RMS.

● **METHODS:** Immunohistochemistry was performed to analyze HPSE-1 expression in 51 cases of orbital RMS patients (including 28 cases of embryonal RMS and 23 cases of alveolar RMS), among whom there were 27 treated and 24 untreated with preoperative chemoradiotherapy. *In vitro*, studies were conducted to examine the effect of HPSE-1 silencing on RMS cell proliferation and tube formation of human umbilical vein endothelial cells (HUVECs). RD cells (an RMS cell line) and HUVECs were infected with HPSE-1 shRNA lentivirus at a multiplicity of infection (MOI) of 10 and 30 separately. Real-time PCR and Western blot were applied to detect the mRNA and protein expression levels of HPSE-1. Cell viability of treated or control RD cells was evaluated by cell counting kit-8 (CCK-8) assay. Matrigel tube formation assay was used to evaluate the effect of HPSE-1 RNAi on the tube formation of HUVECs.

● **RESULTS:** Immunohistochemistry showed that the expression rate of HPSE-1 protein was 92.9% in orbital embryonal RMS and 91.3% in orbital alveolar RMS. Tissue from alveolar orbital RMS did not show relatively stronger staining than that from the embryonal orbital RMS. However, despite the types of RMS, comparing the cases treated chemoradiotherapy with those untreated, we have observed that chemoradiotherapy resulted in weaker staining in patients' tissues. The expression levels of HPSE-1 declined significantly in both the mRNA and protein levels in HPSE-1 shRNA transfected RD cells. The CCK-8 assay showed that lentivirus-mediated HPSE-1 silencing resulted in significantly reduced RD cells viability *in vitro*. Silencing HPSE-1 expression also inhibited VEGF-induced tube formation of HUVECs in Matrigel.

● **CONCLUSION:** HPSE-1 silencing may be a promising therapy for the inhibition of orbital RMS progression.

● **KEYWORDS:** heparanase-1; rhabdomyosarcoma; CCK-8; tube formation; chemoradiotherapy

DOI:10.18240/ijo.2022.01.05

Citation: Tang WQ, Hei Y, Lin J. Heparanase-1 is downregulated in chemoradiotherapy orbital rhabdomyosarcoma and relates with tumor growth as well as angiogenesis. *Int J Ophthalmol* 2022;15(1):31-39

INTRODUCTION

Rhabdomyosarcoma (RMS) is a rare type of soft tissue sarcoma with a high degree of malignancy and mortality[1]. Head and neck RMS occur frequently, and approximately 25%-30% of them appear in the orbit[2-3]. It is well known as a pediatric disease. In adults, its incidence is pretty low, and prognosis is significantly worse, compared with those in children[4-5]. RMS are subdivided into 4 types in the 2013 WHO classification, including embryonal, alveolar, spindle cell/sclerosing, and pleomorphic RMS[6]. Embryonal rhabdomyosarcoma (ERMS) and alveolar rhabdomyosarcoma (ARMS) were the primary histologies. In addition to differences in clinical presentations and outcomes, a number of genetic features separate ARMS from ERMS. The alveolar type is less frequent with a worse prognosis[7-10]. Therefore, histology was considered to be a major treatment determinant and the most important prognostic factor[11]. The commonest embryonal type is significantly correlated with orbital involvement[12]. Excellent prognosis of orbital RMS can be achieved frequently by treatment based on combination chemotherapy together with local surgery therapy and/or

radiation therapy[13-14]. However, local complications are common, including cataract, keratopathy, orbital hypoplasia or fat atrophy, eyelid malposition and lacrimal duct stenosis[15-16]. To minimize ophthalmic adverse effects, novel therapeutic strategies are urgently needed for this malignancy. There are several attractive therapeutic strategies that have been investigated in RMS to date, including those directed against receptor tyrosine kinases and associated downstream signaling pathways, the Hedgehog signaling pathway, apoptosis pathway, DNA damage response, cell-cycle regulators, oncogenic fusion proteins, and epigenetic modifiers[17-18]. Our previous study showed that there is a parallel between over-expression of heparanase-1 (HPSE-1) and key molecules of the Hedgehog signaling pathway in untreated human alveolar orbital RMS[19]. HPSE-1 is the only known mammalian endo-β-glucuronidase that can decompose heparan sulfate proteoglycans (HPSG) within the extracellular matrix (ECM), basement membrane (BM) or on the cellular surface. Its activity has been strongly implicated in cell invasion and migration—a consequence of the structural modification that loosens the ECM barrier[20-22], thereby it is involved in the regulation of multiple cellular processes and biological activities. Unlike matrix metalloproteinases (MMPs) enzyme families, HPSE-1 and its only close homolog HPSE-2 exert opposing biological properties[23-25]. Previous studies have confirmed that elevated expression of HPSE-1 dramatically enhances tumor growth, angiogenesis, and metastasis, and it can be served as an independent prognostic factor for poor outcome of some cancer patients[26]. The heparan sulfate mimetic PI-88 is a complex mixture of sulfated oligosaccharides that was identified as a potent inhibitor of HPSE-1 and subsequently entered clinical trials for cancer. It progressed to Phase III trials but ultimately was not approved for use because of the antibody-induced thrombocytopenia in some patients[27-29]. Advances in the chemistry of the heparan sulfate mimetics PG500 series provide numerous advantages over PI-88. PG545 has been selected as the lead clinical candidate for oncology and is currently undergoing formal preclinical development as a novel treatment for advanced cancer[30-31].

Current knowledge about HPSE-1 mRNA and protein expression in orbital ARMS is only based on our previous report[19]. However, it has not been elucidated whether HPSE-1 protein can be a targeted therapy factor of orbital RMS. In the present study, we examined the expression of HPSE-1 protein levels in ERMS and ARMS specimens, as well as preoperative chemoradiotherapy and untreated patients. Furthermore, the antitumor efficacy of HPSE-1 targeted therapy was investigated *in vitro*. Both RMS cells viability and tube formation of human umbilical vein endothelial cells (HUVECs) induced by vascular endothelial growth factor (VEGF) were evaluated.

MATERIALS AND METHODS

Ethical Approval The use of specimens from human subjects was approved by the Institutional Review Board of Chinese PLA General Hospital, and a signed consent form was obtained from each patient.

Study Subjects Formalin-fixed paraffin-embedded RMS specimens were obtained from 51 patients with orbital RMS, who were aged between 1 and 41y, and surgically treated in the Department of Ophthalmology, the Third Medical Centre, Chinese PLA General Hospital. Among these 51 patients, there were 28 ERMS and 23 ARMS; 27 cases (14 of ERMS and 13 of ARMS) received preoperative chemoradiotherapy followed by surgery (chemotherapy drugs include cyclophosphamide 100-400 mg, vincristine 1-1.5 mg and adriamycin 10-30 mg; The radiation dose is 60 Gy), while the other 24 patients received no such treatment before surgery.

Immunohistochemistry The presence of HPSE-1 protein expression in 28 ERMS and 23 ARMS samples was confirmed by immunohistochemistry. The paraffin embedded tissues were sectioned with 3 μm thick and collected on glass slides, deparaffinized in xylene, and were then rehydrated in a graded ethanol series and washed in phosphate-buffered saline (PBS). The sections were immersed in citrate buffer (pH 6.0), and samples were heated in a pressure cooker for 10min to achieve antigen retrieval of HPSE-1. The rabbit anti-HPSE-1 (1:100; Abcam Ltd., Hong Kong, China.) was used as primary antibody. Sections were reacted with primary antibodies overnight at 4°C and washed three times in PBS, then followed by incubation with secondary anti-rabbit IgG polyclonal antibodies (1:250, Abcam) conjugated to horseradish peroxidase (HRP) for 30min at room temperature. A diaminobenzine (DAB) solution was added at room temperature for 3-5min to illuminate the positive staining signals, and the sections were counterstained with haematoxylin for 20s. Immunostaining results were assessed for intensity and extent by three experienced pathologists. Positive expression was defined as >10% of the cells showing moderate or intense positive cell staining by the antibody in 10 randomly selected fields on every section or >50% of the cells showing weak staining[19].

Cell Culture RD cells (a human RMS cell line), 293T cells and HUVECs were obtained from the cell bank of the Chinese Academy of Science (Shanghai, China) and incubated at 37°C in a humidified atmosphere which was maintained at 5% CO_2.

RD cells and 293T cells were cultured in a mixture containing Dulbecco's modified Eagle's medium (DMEM; Invitrogen, Gaithersburg, MD) supplemented with 100 IU/mL penicillin and 100 μg/mL streptomycin, 1% GlutaMAX and 10% fetal bovine serum (FBS). HUVECs were cultured on ScienCell

Table 1 The primer sequences and length of the PCR products in RT-PCR

Gene	Forward primer (5'-3')	Reverse primer (5'-3')	PCR products (bp)
HPSE-1	ACCATTGACGCCAACCTG	CTGGCCAAGGTACGAAGC	77
Actin	TCCTTCCTGGGCATGGAGT	CAGGAGGAGCAATGATCTTGAT	208

ECM supplemented with 5% FBS, 100 U/mL penicillin, 100 μg/mL streptomycin, 100 μg/mL endothelial cell growth factor.

Construction and Filtering of the Most Effective HPSE-1 shRNA Plasmid Four coding regions in the sequence of human HPSE mRNA (NM_006665.5) were designed as the target sequences. Four pairs of complementary DNA oligos were synthesized and annealed to generate a double-stranded oligo, followed by ligating into the linearized pcDNA6.2-GW/EmGFP-miR vector (Invitrogen, Carlsbad, CA, USA) using T4 DNA ligase at 22°C for 2h. 293T cells with high transfection efficiency of pcDNA6.2-EmGFP negative control plasmid were selected for plasmid transfection. For the relatively low abundance of HPSE-1 gene expression in 293T cells detected by reverse transcription polymerase chain reaction (RT-PCR; Figure 1), we cloned HPSE-1 cDNA into a pEGFP-N1 eukaryotic expression vector (Invitrogen) to construct a HPSE-1 eukaryotic plasmid. Using POLO deliverer™ 3000 (Shanghai R&S Biotechnology Co., Ltd., Shanghai, China) according to the manufacturer's instruction, the HPSE-1 eukaryotic plasmid was then co-transfected with the recombinant vectors with HPSE-1 shRNA1, HPSE-1 shRNA2, HPSE-1 shRNA3, HPSE-1 shRNA4 (targeting different sequences of HPSE-1) or the Neg-shRNA into 293T cells, respectively. HPSE-1 mRNA and protein expressions were detected by RT-PCR and Western blotting to filter out the most effective vector with HPSE-1 shRNA.

Construction of the HPSE-1 shRNA Lentivirus Vector Sequences of the most effective HPSE-1 shRNA were inserted into the pLenti6.3/V5 DEST™ lentivirus RNAi expression system (Invitrogen, Carlsbad, CA, USA) to construct the HPSE-1 shRNA lentivirus vector. The insert was cloned into the pLenti6.3/V5 DEST plasmid by double digesting with AscI/PmeI enzymes and ligating with T4 DNA ligase. The resulting pLenti6.3-HPSE-1 shRNA was then sequenced and co-transfected with the ViraPower™ Lentiviral Packaging Mix (Invitrogen) using POLO deliverer™ 3000 (Shanghai R&S Biotechnology Co., Ltd.) into 293T cells. Viral supernatant was harvested 72h post-transfection and titers were determined by the green fluorescent protein (GFP) assay of the 293T cells infected with serial dilutions of concentrated lentivirus.

HPSE-1 shRNA Recombinant Lentiviral Transduction RMS cells were randomly divided into 3 different groups, which were transfected with HPSE-1 shRNA (Inhibition group), Neg-shRNA (Negative control group), or untreated (blank cell group). The recombinant lentiviruses with HPSE-1 shRNA were transduced into RD cells with an optimized multiplicity of infection (MOI=10). Appropriate amount of HPSE-1 shRNA lentiviruses (2.745×10^8 TU/mL) and negative control lentiviruses (2.0×10^8 TU/mL) were added into the cells, 4-8 μg/mL polybrene was also added to enhance the infection. The expression of lentivirus GFP was observed under fluorescence microscope 72h after infection and the percentage of fluorescent cells was more than 85%, which can be used for subsequent experiments.

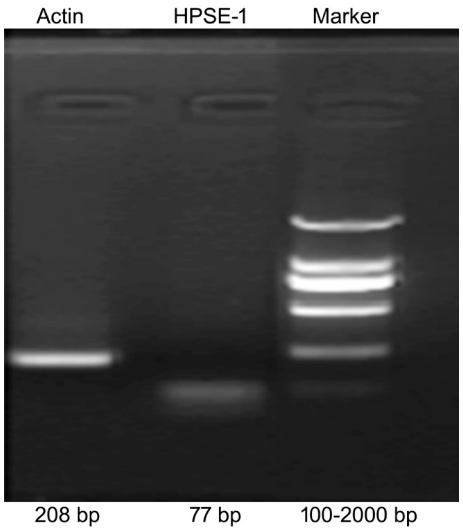

Figure 1 HPSE-1 mRNA expression in 293T cells *via* RT-PCR showed low abundance.

HPSE-1 mRNA and Protein Levels in RD Cells *in vitro*

Quantitative real-time PCR Total RNA was extracted from RD cells using Trizol (Invitrogen). The concentration and purity of RNA was subjected for a spectrophotometer analysis (Fullertone, CA, USA). RNA was reversely transcribed using M-MLV reverse transcriptase (Fermentas Inc., Burlington, Canada) at a total volume of 20 μL according to the manufacturer's instructions. Subsequently, the qPCR assay was carried out using 2×SYBR Green qPCR Mix (Invitrogen) at the real-time PCR amplification equipment of mastercycler EP realplex (Eppendorf AG, Hamburg, Germany). The PCR primers used to detect HPSE-1 and β-actin mRNA expression were seen in Table 1. PCR conditions included an initial step of 95℃ for 2min, followed by 40 cycles of 95℃ for 20s and then annealed at 60℃ for 15s, and 72℃ for 20s. Products were identified by melting curve analysis after 39 cycles. The comparative Ct ($^{\Delta\Delta}$Ct) method was used to calculate the relative quantitation of mRNA as previously described[23]. The

expression of HPSE-1 was determined by normalization of the threshold cycle (Ct) of HPSE-1 gene to that of β-actin. The ΔCt and ΔΔCt were determined using the following equation: ΔCt = (Ct of HPSE-1) - (Ct of β-actin), ΔΔCt = (mean ΔCt of HPSE-1 genes in RNAi groups) - (ΔCt of HPSE-1 genes in control group). The $2^{-\Delta\Delta Ct}$ implicates the relative expression vaule of the HPSE-1 gene.

Western blotting After washed two times with PBS at room temperature, the protein was extracted from RD cells using cell lysis buffer containing phenylmethanesulfonyl fluoride (PMSF; Sigma-Aldrich, Shanghai, China). The protein concentrations were determined by bicinchonic acid (Sigma-Aldrich) protein assay. Samples were separated by 10% sodium dodecyl sulfate (SDS)-polyacrylamide gel electrophoresis (PAGE), and then the proteins were electro-transferred with a semi-dry blotting system onto a polyvinylidene fluoride (PVDF) membrane. The membrane was blocked with 5% non-fat milk in Tris-buffered saline (TBS) for one hour at room temperature, followed by hybridization with the primary antibody overnight at 4°C. The primary antibody included the HPSE-1 antibody (Abcam, Cambrideg, UK) at a dilution of 1:1000 and the GADPH antibody (Bioworld Technology, CA, USA) at a dilution of 1:5000. After washed three times with TBS/0.1% Tween 20 for 30min, a corresponding secondary antibody was added to the membrane (1:5000 dilution, Santa Cruz Biotechnology) for 1h at room temperature. Subsequently, after 3 washes in TBS/0.1% Tween 20 for 30min, the signals were visualized by a chemiluminescence reagent (Thermo Fisher Scientific, MA, USA) followed by exposure to X-ray film. All experiments were repeated three times.

Human Rhabdomyosarcoma Cells Viability Assay The proliferation of RD cell lines was evaluated by cell counting kit-8 (CCK-8) assay. RD Cells were seeded in 96-well culture plates at a density of 4000 cells per well. After the cells were transfected with the recombinant lentivirus at an MOI of 10 for 12h, the medium was replaced with a fresh complete medium. Blank cells and silenced cells were tested as well as the relative negative controls. After 24h incubation, 10 μL of CCK-8 solution was added to each well for an additional 3h at 37°C. The number of proliferating cells was evaluated by measuring the absorbance at a 450 nm wavelength on a microtiter plate reader (Thermo Fisher Scientific, MA, USA) at the same time of 6 continuous days, and cellular viability was evaluated by the A_{450nm} value.

Tube Formation Assay Basement membrane extracellular matrix (Matrigel; BD Biosciences, San Jose, CA, USA) was thawed at 4°C overnight. The 200 μL pipette tips and a 96-well plate were also kept at 4°C overnight. Matrigel (90 μL) was loaded in each well, and then the plate was incubated at 37°C for 30min to solidify the matrix. The appropriate amount of recombinant lentivirus containing HPSE-1 shRNA (1×10^8 TU/mL) and negative control lentivirus (1×10^8 TU/mL) were added into the cells (MOI=30), and the final concentration of polybrene was 8 μg/mL. After infection 48h, the pretreated HUVECs were seeded on the solidified matrigel at a density of 10^4 cells/well. The plates were kept at room temperature for 15min and then transferred to the 5% CO_2 incubator at 37°C. The capillary-like structure formation of HUVECs was observed at different time points during a 12h experimental period using a microscope. After incubation for 4, 6, and 10h, the capillary-like tube formation was quantified by counting the length of tubes in 5 randomly selected optical fields using an Olympus microscope (Olympus Corporation, Tokyo, Japan).

Statistical Analysis Data were collected and expressed as the mean±standard error (SD) and were analysed using SPSS statistical software (Ver 11.0, Chicago, IL, USA) with differences between groups assessed by Student's *t* test or one-way analysis of variance (ANOVA). $P<0.05$ was considered significant.

RESULTS

Immunohistochemistry HPSE-1 protein expression was examined in 28 orbital ERMS and 23 orbital ARMS by immunohistochemistry. Positive expression was observed with different staining intensity in 92.9% of embryonal samples and 91.3% of alveolar samples tested and primarily located in the cytoplasm and nucleus. Generally speaking, there was no significant difference in HPSE-1 immunostaining intensity between ERMS and ARMS specimens. However, both of them displayed the similar tendency. Tissue from untreated (no chemoradiotherapy before surgery) RMS patients tended to show intense staining, whereas tissue from RMS patients treated with chemoradiotherapy (chemoradiotherapy followed by surgery) showed relatively weaker staining (Figure 2).

Most Effective HPSE-1 shRNA Plasmid was Singled Out Four recombinant plasmids of HPSE-1 shRNA (1-4), targeting four different encoding regions of HPSE-1 mRNA, were successfully constructed using pcDNA6.2-GW/EmGFP-miR, which were confirmed by DNA sequence analysis. Forty-eight hours after the co-transfection of HPSE-1 shRNA plasmid and HPSE-1 eukaryotic expression vector, 293T cells were divided into six groups, *i.e.*, HPSE-1 shRNA1-4, negative control, and blank cells group. All the four recombinant plasmids of HPSE-1 shRNA successfully down-regulated HPSE-1 mRNA and protein expression levels, and the plasmid with HPSE-1 shRNA1 was shown to be the most efficient RNAi vector. Compared with negative control group, HPSE-1 mRNA and protein expression levels in 293T cells that were transfected with HPSE-1 shRNA1 were down-regulated by maximum 95% (RT-qPCR) and 58.3% (Western blotting) respectively (Figure 3).

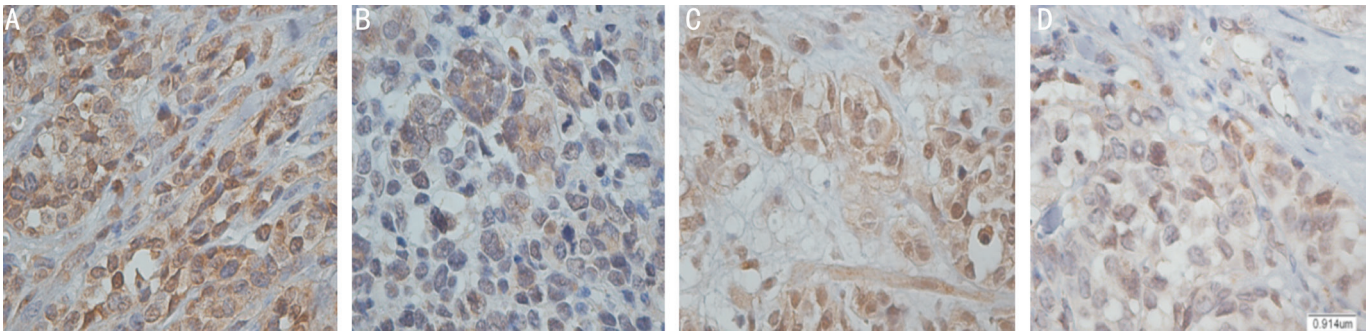

Figure 2 Expression of heparanase-1 protein in the embryonal and alveolar orbital rhabdomyosarcoma HPSE-1 positive staining were seen in the samples obtained from embryonal orbital RMS (A, B) and alveolar orbital RMS (C, D). A, C: No chemoradiotherapy before surgery; B, D: Chemoradiotherapy followed by surgery. Samples tended to stain intensely in A and C, but staining was relatively weak in B and D.

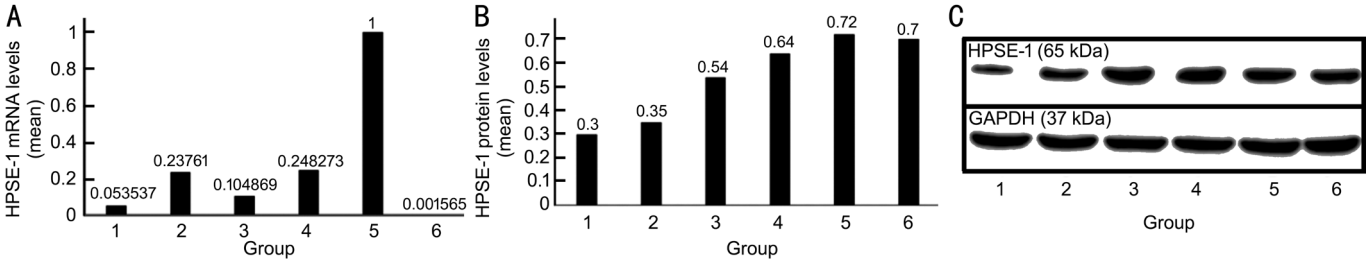

Figure 3 HPSE-1 eukaryotic plasmid was co-transfected with four recombinant plasmid of HPSE-1 shRNA1, 2, 3, 4 into 293T cells respectively HPSE-1 mRNA and protein expressions were detected by RT-qPCR and Western blotting to filter out the most effective HPSE-1 shRNA plasmid. Group 1-4: HPSE-1 shRNA (1-4) + HPSE-1 eukaryotic plasmid transfected group; Group 5: Negative control + HPSE-1 eukaryotic plasmid transfected group; Group 6: Blank control group. The plasmid of HPSE-1 shRNA1 attained the most inhibition effect of HPSE-1 mRNA (A) and protein levels (B, C).

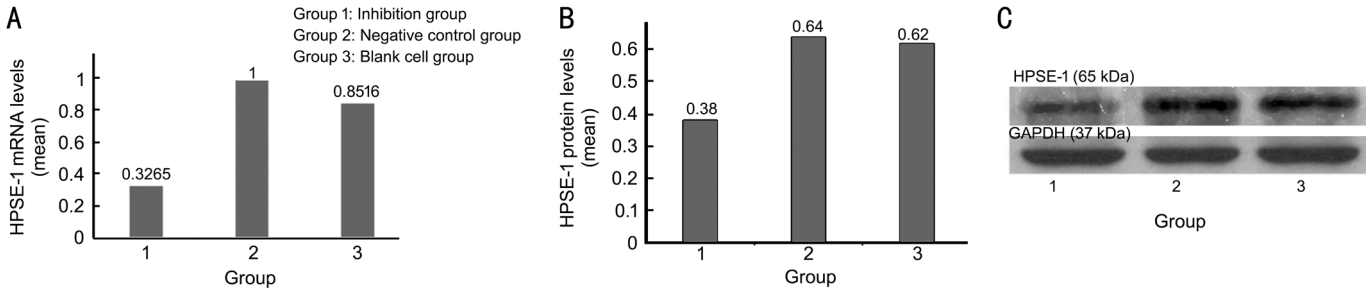

Figure 4 The pLenti6.3-HPSE-1 shRNA recombinant lentivirus was construced and transduced into RD cells A: HPSE mRNA expression levels in control (group 2, 3) and silenced (group 1) RD cell lines were determined by real-time PCR. The results were normalized using β-actin as internal control. B, C: Western blot analysis was performed to demonstrate HPSE-1 silencing between control and silenced RD cell lines. GAPDH was included as loading control. HPSE-1 mRNA and protein expression in RD cells were compared between inhibition group, negative control group, and blank cell group. The average HPSE-1 mRNA and protein levels were downregulated by 67% (A) and 41% (B) in the inhibition group of RD cells infected with HPSE-1 shRNA recombinant lentivirus compared to that of negative control group respectively (P<0.05).

Construction of the pLenti6.3-HPSE-1 shRNA Lentivirus Vector The HPSE-1 shRNA1 was used as the foundation for construction of the pLenti6.3-HPSE-1 RNAi lentivirus vector. Lentiviral vectors was packaged in 293T cells and the GFP expression was observed 72h post-package under the fluorescence microscope, the viral titer was calculated to be 2.75×10^8 TU/mL. Recombinant lentiviruses with HPSE-1 shRNA were transduced into RD cells and the levels of HPSE-1 mRNA and protein were tested by real-time RT-qPCR and Western blotting in three groups of RD cells (inhibition group, negative control group, and blank cell group). As shown in Figure 4, HPSE-1 mRNA and protein expressions in the inhibition group were decreased by 67% and 41% respectively, when compared with the negative control group (P<0.05). The lentivirus-mediated HPSE-1 RNAi notably down-regulated HPSE-1 expression levels of both mRNA and protein in RD cells.

Lentivirus-mediated HPSE-1 RNAi Attenuated RD Cellular Proliferation The optical density (OD) value of viable RD cells in different groups were determined by CCK-8 assay. The results showed that RD cells, transfected stably with

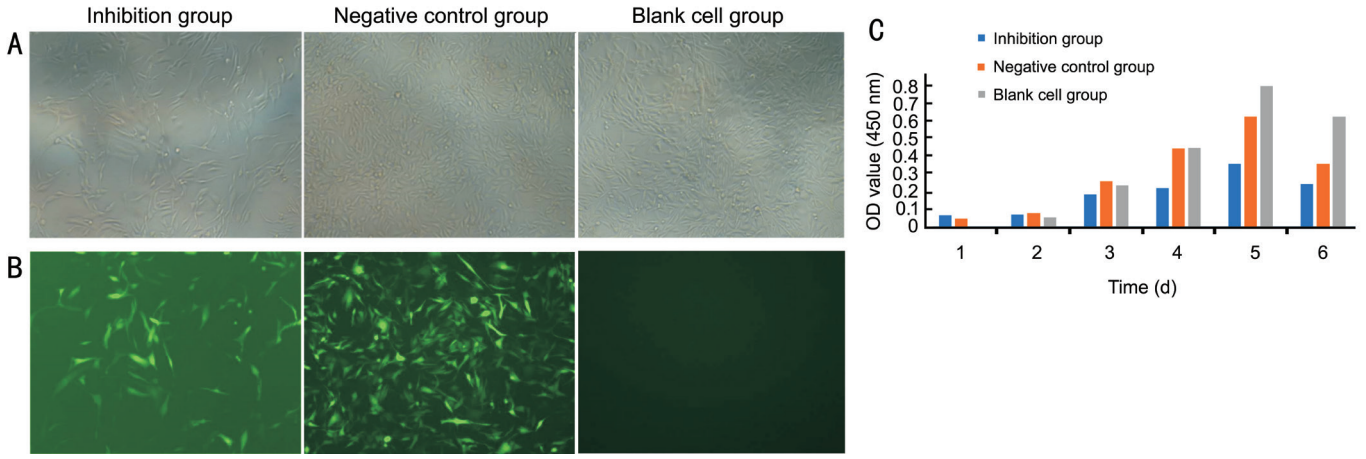

Figure 5 Effects of lentivirus-mediated HPSE-1 shRNA on RD cells proliferation RD cells infected with HPSE-1 shRNA recombinant lentivirus (inhibition group) or negative control lentivirus (negative control group) and blank RD cells (blank cell group) were cultured for 6d consecutively. Five days after treatment, RD cells proliferation were observed under microscope (A) and fluorescence microscope (B; ×10). C: Average OD values of different treated RD cells were analysed using CCK-8 assay.

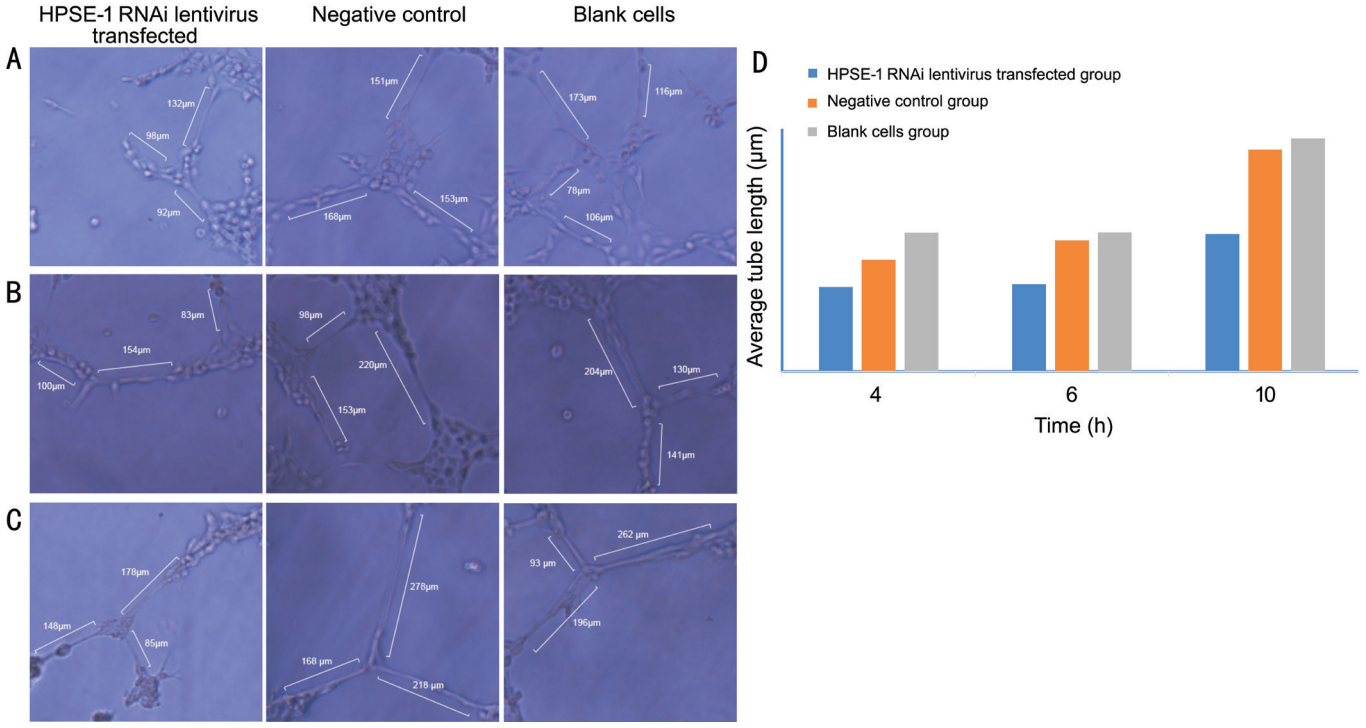

Figure 6 VEGF-containing serum induced tube formation Counting results of tube length, HPSE-1 RNAi lentivirus transfected group compared with negative control group and blank cells group at 4h (A), 6h (B), and 10h (C) after incubation. D: Average tube length of HPSE-1 RNAi lentivirus transfected group decreased compared with negative control group or blank cells group.

HPSE-1 shRNA, had reduced viability when compared to the blank cells or the negtive-shRNA transfected cells at 3, 4, 5, and 6d, the A_{450nm} values of HPSE-1 shRNA transfected cells were significantly lower than control groups (P<0.05; Figure 5, Table 2).

Lentivirus-mediated HPA-1 RNAi Inhibited the Tube Formation of HUVECs Compared with blank cell group and negative control group, the average tube length in HPSE-1 RNAi lentiviral infection group was significantly shorter (P<0.05), which suggested that down-regulated HPSE-1 expression can inhibit the tube formation of HUVEC cells (Figure 6, Table 3).

DISCUSSION

In the present study, HPSE-1 protein was expressed in 92.9% of the orbital ERMS specimens and in 91.3% of orbital ARMS ones. The staining intensity of the alveolar type was not stronger than that of the embryonic type. However, tissue from untreated RMS patients tended to show stronger staining than that from chemoradiotherapy patients. *In vitro*, when

Table 2 A_{450} value of RD cells were analysed using CCK-8 assay *n*=6, mean±SD

Group	1d	2d	3d	4d	5d	6d
A	0.071±0.013	0.076±0.019	0.189±0.036[a,b]	0.225±0.027[a,b]	0.361±0.030[a,b]	0.246±0.021[a,b]
B	0.052±0.017	0.084±0.024	0.262±0.023	0.449±0.033	0.629±0.040	0.363±0.031
C	0.005±0.001	0.058±0.019	0.238±0.034	0.454±0.028	0.801±0.029	0.630±0.027

Group A: HPSE-1 miRNA lentivirus transfected; Group B: Negative control; Group C: Blank cells. [a]*P*<0.05, A versus B group; [b]*P*<0.05, A versus C group.

Table 3 The average tube length in three groups after HUVEC incubated in matrige mean±SD, μm

Group	4h (*n*)	6h (*n*)	10h (*n*)
A	102.64±25.66[a,b] (10)	106.17±30.42[a,b] (7)	167±41.64[a,b] (5)
B	135.58±38.4 (8)	159.28±49.32 (7)	269.56±68.85 (5)
C	168.61±18.43 (9)	168.78±52.12 (7)	283.11±76.48 (5)

Group A: HPSE-1 miRNA lentivirus transfected; Group B: Negative control; Group C: Blank cells. [a]*P*<0.05, A versus B group; [b]*P*<0.05, A versus C group.

HPSE-1 shRNA recombinant lentivirus was successfully constructed and transfected into RMS cells, the expression of HPSE-1 mRNA and protein levels decreased by 67% and 41% respectively compared with RMS cells infected with negative control lentivirus. Transfection of lentivirus-mediated HPSE-1 shRNA induces decreased RMS cell proliferation after 72h incubation by CCK-8 assay. In addition, lentivirus mediated HPSE-1 shRNA silenced the expression of HPSE-1 gene in HUVEC cells, which significantly inhibited VEGF induced angiogenesis. In our study, HUVECs were cultured on the ECM supplemented with 100 μg/mL endothelial cell growth factor.

RMS is a highly malignant soft-tissue tumor of childhood and adolescence that arises in the skeletal muscle, and approximately 10% of the total tumors occur in the orbit. Many clinical association studies have consistently demonstrated that the embryonal type is the most common variant; alveolar variant is less frequent but has a worse prognosis[32-33]. Increased expression of HPSE-1 has been observed in numerous malignancies and is associated with a poor prognosis[34-35]. Furthermore, it has been well recognized that HPSE-1 weakly expresses in normal human tissues and its elevated levels are associated with increased tumor angiogenesis and metastasis[22,30,36-37]. In our study, the paraffin samples consisted of 28 ERMS and 23 ARMS. However, the expression of HPSE-1 protein in ARMS with worse prognosis was not stronger than that in ERMS. This has not been consistent. In two groups, tissue from untreated RMS patients tended to show stronger staining. Our previous study has also demonstrated chemotherapy and/or radiotherapy appears to significantly inhibit HPSE-1 upregulation in orbital RMS[19].

In order to determine the HPSE-1 role in the progression and metastasis potential of orbital RMS, we stably silenced RD cell line by lentiviral vectors-mediated HPSE-1 shRNA *in vitro*. RNAi has been widely used since its first discovery in 1998, and lentiviral vectors-mediated RNAi is known to be able to induce a stable and long-term gene silencing in both dividing and non-dividing cells[27,38]. Based on the real-time RT-qPCR and Western blotting assay results, from four designed HPSE-1 shRNA vectors, we selected one that was characterized with the most HPSE-1 silence efficiency, in order to construct the HPSE-1 shRNA recombinant lentivirus. After transducing into RMS cells, HPSE-1 mRNA and protein levels appeared to be silenced obviously. We demonstrated that HPSE-1 silencing significantly reduced the proliferation potential of RD cell lines compared with the untreated cells. Because Masola *et al*[39] have demonstrated in RD cell lines that no change in cell proliferation was observed by MTT analysis after HPSE-1 silencing, we determined the effects of HPSE-1 silencing in RD cell proliferation by analyzing A_{450nm} values for 6 consecutive days using CCK-8 assay. In our cellular model we observed the inhibition phenomenon of cell proliferation at different time points (from 3 to 6d) in HPSE-1 silenced RD cells and in blank or negative control RD cells. Our data suggests that HPSE-1 presumably serves as an oncogenic gene for RMS cells.

Angiogenesis is a crucial step for cancer metastasis; the formation of new networks of blood vessels from pre-existing vessels creates a favorable microenvironment during cancer progression[40]. HPSE-1 can release heparan sulfate bound proangiogenic growth factors (bFGF, HGF, PDGF and VEGF) from the ECM to promote endothelial cell proliferation and to facilitate the remodeling of the extracellular matrix prior to ECM during angiogenesis. Thus, tumors with elevated HPSE-1 levels have significantly higher microvessel density than tumors with low HPSE-1 expressions[41]. It had been reported that HPSE-1 and VEGF are positively correlated in human adrenocortical carcinoma and their expressions

were positively correlated with microvessel density in all specimens[42]. VEGF is known to be a key angiogenic factor and plays a crucial role in cancer development through the regulation of angiogenesis[43-44]. To further study the effect of HPSE-1 on angiogenesis of orbital RMS, we *in vitro* invested whether the application of specific RNAi targeting HPSE-1 is effective in inhibiting VEGF induced HUVECs tube formation. Our data revealed a definite inhibiting effect of HPSE-1 silencing on angiogenesis. *In vitro*, HUVEC cells that were transfected with lentivirus mediated HPSE-1 shRNA showed significantly reduced ability of tube formation. This is consistent with the result obtained in a previous study, which showed HPSE-2 functions as an inhibitor of the HPSE-1 enzyme and also inhibits neovascularization mediated by VEGF[45].

In summary, the positive immunohistochemical overexpression of HPSE-1 proteins in specimens advocates that HPSE-1 may possibly play some role in the growth of the orbital RMS. Also, we have observed promising results about HPSE-1 gene silencing on RMS cell proliferation and angiogenesis. A previous study has indicated that the expression level of HPSE-1 in normal human tissues is rather low, and there is no obvious abnormality in HPSE-1 gene knockout animals[23]. All these dates emphasize the therapeutic potential of anti-HPSE-1 therapy for orbital RMS. Therefore, HPSE-1 gene silencing may be developed as a novel therapy to prevent the progression of orbital RMS without sacrificing patients' quality of life. Further research is needed to establish the animal model of orbital RMS, and to study the effect of HPSE-1 silencing on tumor growth *in vivo*. Moreover, significant differences in the survival rates of ERMS and ARMS have been demonstrated[46]. The correlation between HPSE-1 expressions and survival rates of different types of RMS was not discussed in the current study, and it requires further investigation.

ACKNOWLEDGEMENTS

Conflicts of Interest: Tang WQ, None; **Hei Y,** None; **Lin J,** None.

REFERENCES

1 Kerin Ú, Wolohan C, Cooke K. Rhabdomyosarcoma: an overview and nursing considerations. *Br J Nurs* 2018;27(6):328-332.

2 Morales RL, Álvarez A, Esguerra J, Prada Avella MC, Rojas F. Primary conjunctival rhabdomyosarcoma in a pediatric patient. *Cureus* 2019;11(12):e6310.

3 Chen E, Ricciotti R, Futran N, Oda D. Head and neck rhabdomyosarcoma: clinical and pathologic characterization of seven cases. *Head Neck Pathol* 2017;11(3):321-326.

4 Ruiz-Mesa C, Goldberg JM, Coronado Munoz AJ, Dumont SN, Trent JC. Rhabdomyosarcoma in adults: new perspectives on therapy. *Curr Treat Options Oncol* 2015;16(6):27.

5 Drabbe C, Benson C, Younger E, Zaidi S, Jones RL, Judson I, Chisholm J, Mandeville H, Fisher C, Thway K, Al Muderis O, Messiou C, Strauss D, Husson O, Miah A, van der Graaf WTA. Embryonal and alveolar rhabdomyosarcoma in adults: real-life data from a tertiary sarcoma centre. *Clin Oncol* (*R Coll Radiol*) 2020;32(1):e27-e35.

6 Leiner J, Le Loarer F. The current landscape of rhabdomyosarcomas: an update. *Virchows Arch* 2020;476(1):97-108.

7 Unsal AA, Chung SY, Unsal AB, Baredes S, Eloy JA. A population-based analysis of survival for sinonasal rhabdomyosarcoma. *Otolaryngol Head Neck Surg* 2017;157(1):142-149.

8 Lacey A, Rodrigues-Hoffman A, Safe S. PAX3-FOXO1A expression in rhabdomyosarcoma is driven by the targetable nuclear receptor NR4A1. *Cancer Res* 2017;77(3):732-741.

9 Parham DM, Barr FG. Classification of rhabdomyosarcoma and its molecular basis. *Adv Anat Pathol* 2013;20(6):387-397.

10 Li H, Sisoudiya SD, Martin-Giacalone BA, Khayat MM, Dugan-Perez S, Marquez-Do DA, Scheurer ME, Muzny D, Boerwinkle E, Gibbs RA, Chi YY, Barkauskas DA, Lo T, Hall D, Stewart DR, Schiffman JD, Skapek SX, Hawkins DS, Plon SE, Sabo A, Lupo PJ. Germline cancer predisposition variants in pediatric rhabdomyosarcoma: a report from the children's oncology group. *J Natl Cancer Inst* 2021;113(7):875-883.

11 Iatrou I, Theologie-Lygidakis N, Schoinohoriti O, Tzermpos F, Vessala AM. Rhabdomyosarcoma of the maxillofacial region in children and adolescents: report of 9 cases and literature review. *J Craniomaxillofac Surg* 2017;45(6):831-838.

12 Albalawi ED, Alkatan HM, Elkhamary SM, Safieh LA, Maktabi AMY. Genetic profiling of rhabdomyosarcoma with clinicopathological and radiological correlation. *Can J Ophthalmol* 2019;54(2):247-257.

13 Boutroux H, Levy C, Mosseri V, Desjardins L, Plancher C, Helfre S, Freneaux P, Cellier C, Orbach D. Long-term evaluation of orbital rhabdomyosarcoma in children. *Clin Exp Ophthalmol* 2015;43(1):12-19.

14 Schoot RA, Saeed P, Freling NJ, Blank LE, Pieters BR, van der Grient JN, Strackee SD, Bras J, Caron HN, Merks JH, Amsterdam Head and Neck Working Group on Childhood Tumors. Local resection and brachytherapy for primary orbital rhabdomyosarcoma: outcome and failure pattern analysis. *Ophthalmic Plast Reconstr Surg* 2016;32(5):354-360.

15 Bravo-Ljubetic L, Peralta-Calvo J, Larrañaga-Fragoso P, Pascual NO, Pastora-Salvador N, Gomez JA. Clinical management of orbital rhabdomyosarcoma in a referral center in Spain. *J Pediatr Ophthalmol Strabismus* 2016;53(2):119-126.

16 Eade E, Tumuluri K, Do H, Rowe N, Smith J. Visual outcomes and late complications in paediatric orbital rhabdomyosarcoma. *Clin Exp Ophthalmol* 2017;45(2):168-173.

17 Saltzman AF, Cost NG. Current treatment of pediatric bladder and prostate rhabdomyosarcoma. *Curr Urol Rep* 2018;19(1):11.

18 van Erp AEM, Versleijen-Jonkers YMH, van der Graaf WTA, Fleuren EDG. Targeted therapy-based combination treatment in rhabdomyosarcoma. *Mol Cancer Ther* 2018;17(7):1365-1380.

19 Tang WQ, Hei Y, Kang L, Xiao LH. Heparanase-1 and components of the hedgehog signalling pathway are increased in untreated alveolar orbital rhabdomyosarcoma. *Clin Exp Ophthalmol* 2014;42(2):182-189.

20 Jin H, Cui M. New advances of heparanase and heparanase-2 in human diseases. *Arch Med Res* 2018;49(7):423-429.

21 Najafi M, Farhood B, Mortezaee K. Extracellular matrix (ECM) stiffness and degradation as cancer drivers. *J Cell Biochem* 2019; 120(3):2782-2790.

22 Barbosa GO, Cervigne NK, Carvalho HF, Augusto TM. Heparanase 1 involvement in prostate physiopathology. *Cell Biol Int* 2017;41(11): 1194-1202.

23 Sanderson RD, Elkin M, Rapraeger AC, Ilan N, Vlodavsky I. Heparanase regulation of cancer, autophagy and inflammation: new mechanisms and targets for therapy. *FEBS J* 2017;284(1):42-55.

24 Vlodavsky I, Gross-Cohen M, Weissmann M, Ilan N, Sanderson RD. Opposing functions of heparanase-1 and heparanase-2 in cancer progression. *Trends Biochem Sci* 2018;43(1):18-31.

25 Kayal Y, Singh P, Naroditsky I, Ilan N, Vlodavsky I. Heparanase 2 (Hpa2) attenuates the growth of pancreatic carcinoma. *Matrix Biol* 2021;98: 21-31.

26 Jiao WJ, Chen YJ, Song HJ, Li D, Mei H, Yang F, Fang EH, Wang XJ, Huang K, Zheng LD, Tong QS. HPSE enhancer RNA promotes cancer progression through driving chromatin looping and regulating hnRNPU/p300/EGR1/HPSE axis. *Oncogene* 2018;37(20):2728-2745.

27 Khanna M, Parish CR. Heparanase: historical aspects and future perspectives. *Adv Exp Med Biol* 2020;1221:71-96.

28 Chhabra M, Ferro V. PI-88 and related heparan sulfate mimetics. *Adv Exp Med Biol* 2020;1221:473-491.

29 Kudchadkar R, Gonzalez R, Lewis KD. PI-88: a novel inhibitor of angiogenesis. *Expert Opin Invest Drugs* 2008;17(11):1769-1776.

30 Dredge K, Hammond E, Davis K, Li CP, Liu L, Johnstone K, Handley P, Wimmer N, Gonda TJ, Gautam A, Ferro V, Bytheway I. The PG500 series: novel heparan sulfate mimetics as potent angiogenesis and heparanase inhibitors for cancer therapy. *Invest New Drugs* 2010;28(3):276-283.

31 Weissmann M, Bhattacharya U, Feld S, Hammond E, Ilan N, Vlodavsky I. The heparanase inhibitor PG545 is a potent anti-lymphoma drug: mode of action. *Matrix Biol* 2019;77:58-72.

32 Ahmad TY, Al Houri HN, Al Houri AN, Ahmad NY. Aggressive orbital rhabdomyosarcoma in adulthood: a case report in a public hospital in Damascus, Syria. *Avicenna J Med* 2018;8(3):110-113.

33 Cortes Barrantes P, Jakobiec FA, Dryja TP. A review of the role of cytogenetics in the diagnosis of orbital rhabdomyosarcoma. *Semin Ophthalmol* 2019;34(4):243-251.

34 Sun X, Zhang GL, Nian JY, Yu MW, Chen SJ, Zhang Y, Yang GW, Yang L, Cheng PY, Yan C, Ma YF, Meng H, Wang XM, Li JP. Elevated heparanase expression is associated with poor prognosis in breast cancer: a study based on systematic review and TCGA data. *Oncotarget* 2017;8(26):43521-43535.

35 Arvatz G, Weissmann M, Ilan N, Vlodavsky I. Heparanase and cancer progression: new directions, new promises. *Hum Vaccin Immunother* 2016;12(9):2253-2256.

36 Tripathi K, Ramani VC, Bandari SK, Amin R, Brown EE, Ritchie JP, Stewart MD, Sanderson RD. Heparanase promotes myeloma stemness and *in vivo* tumorigenesis. *Matrix Biol* 2020;88:53-68.

37 Mohan CD, Hari S, Preetham HD, Rangappa S, Barash U, Ilan N, Nayak SC, Gupta VK, Basappa, Vlodavsky I, Rangappa KS. Targeting heparanase in cancer: inhibition by synthetic, chemically modified, and natural compounds. *iScience* 2019;15:360-390.

38 Masola V, Zaza G, Gambaro G, Franchi M, Onisto M. Role of heparanase in tumor progression: molecular aspects and therapeutic options. *Semin Cancer Biol* 2020;62:86-98.

39 Masola V, Maran C, Tassone E, Zin A, Rosolen A, Onisto M. Heparanase activity in alveolar and embryonal rhabdomyosarcoma: implications for tumor invasion. *BMC Cancer* 2009;9:304.

40 Cheng HW, Chen YF, Wong JM, Weng CW, Chen HY, Yu SL, Chen HW, Yuan A, Chen JJ. Cancer cells increase endothelial cell tube formation and survival by activating the PI3K/Akt signalling pathway. *J Exp Clin Cancer Res* 2017;36(1):27.

41 Heyman B, Yang YP. Mechanisms of heparanase inhibitors in cancer therapy. *Exp Hematol* 2016;44(11):1002-1012.

42 Xu YZ, Zhu Y, Shen ZJ, Sheng JY, He HC, Ma G, Qi YC, Zhao JP, Wu YX, Rui WB, Wei Q, Zhou WL, Xie X, Ning G. Significance of heparanase-1 and vascular endothelial growth factor in adrenocortical carcinoma angiogenesis: potential for therapy. *Endocrine* 2011;40(3): 445-451.

43 Matsumoto K, Ema M. Roles of VEGF-A signalling in development, regeneration, and tumours. *J Biochem* 2014;156(1):1-10.

44 Siveen KS, Prabhu K, Krishnankutty R, Kuttikrishnan S, Tsakou M, Alali FQ, Dermime S, Mohammad RM, Uddin S. Vascular endothelial growth factor (VEGF) signaling in tumour vascularization: potential and challenges. *Curr Vasc Pharmacol* 2017;15(4):339-351.

45 Pinhal MAS, Melo CM, Nader HB. The good and bad sides of heparanase-1 and heparanase-2. *Adv Exp Med Biol* 2020;1221:821-845.

46 Amer KM, Thomson JE, Congiusta D, Dobitsch A, Chaudhry A, Li M, Chaudhry A, Bozzo A, Siracuse B, Aytekin MN, Ghert M, Beebe KS. Epidemiology, incidence, and survival of rhabdomyosarcoma subtypes: SEER and ICES database analysis. *J Orthop Res* 2019; 37(10):2226-2230.